Supporting Information for

High-Throughput Graphene Imaging on Arbitrary Substrates with Widefield Raman Spectroscopy

Robin W. Havener[1,§], Sang-Yong Ju[2,3,§], Lola Brown[2], Zenghui Wang[2], Michal Wojcik[2], Carlos S. Ruiz-Vargas[1], and Jiwoong Park[2,4,]*

1 Department of Applied and Engineering Physics, Cornell University, Ithaca, New York, 14853, 2 Department of Chemistry and Chemical Biology, Cornell University, Ithaca, New York 14853, 3 Department of Chemistry, Yonsei University, Seoul 120-749, Republic of Korea, and 4 Kavli Institute at Cornell for Nanoscale Science, Cornell University, Ithaca, New York 14853

§ These authors contributed equally to this work.

* Correspondence e-mail: jpark@cornell.edu

Contents

Setup of Widefield Raman Imaging

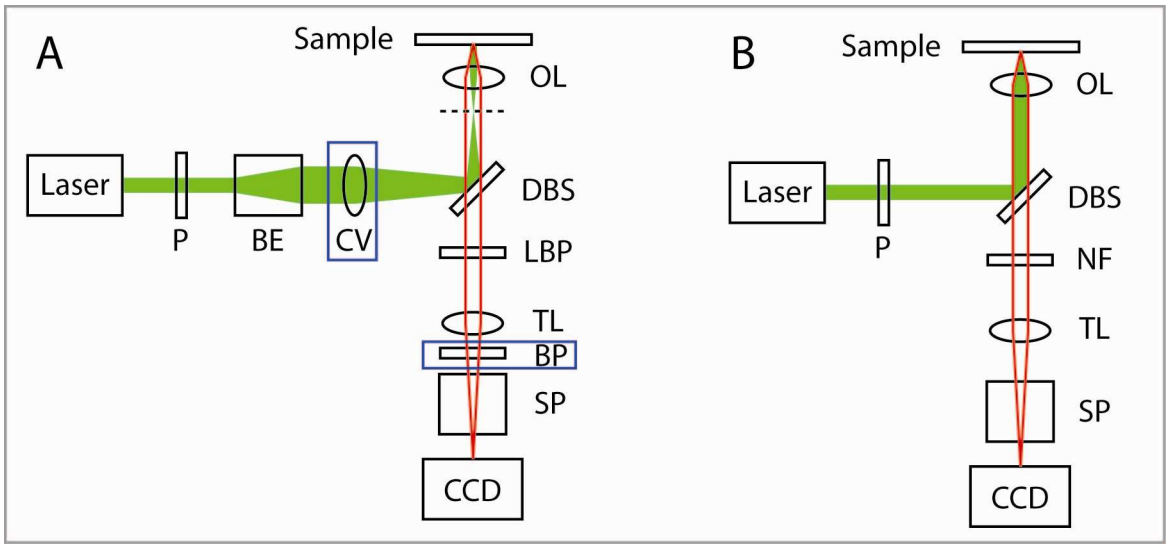

Figure S1: Schematics of widefield Raman setup (A) compared with a typical micro-Raman setup (B). Green and red lines indicate beam profiles of excitation and scattered light, respectively. BP in Figure S1A can be either tunable bandpass filter or single bandpass filter. Abbreviations: P: Polarizer, BE: beam expander, CV: convex lens, DBS: dichroic beam splitter, OL: objective lens, LBP: long bandpass filter, TBP: tunable bandpass filter, CCD: charge-coupled device, NF: notch filter, TL: tube lens, SP: spectrometer. Blue boxes indicate major difference in the configurations of (A) and (B).

Design of tunable bandpass filter

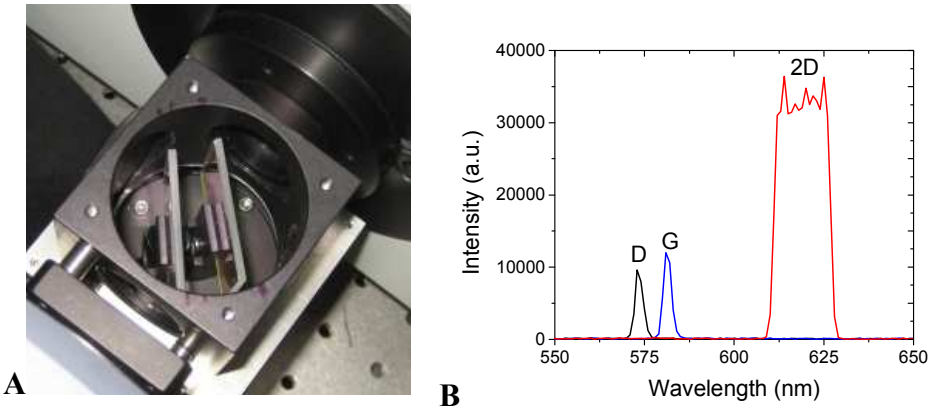

Figure S2: (A) Picture of tunable bandpass filter. Note that the angles of the two bandpass filters are offset slightly. (B) Bandwidth at wavelengths corresponding to D, G, and 2D bands (for 532 nm excitation) obtained from tunable bandpass filter.

Image processing

The Raman intensity is proportional to laser intensity, which is not constant, but roughly Gaussian over the sample surface. Images are *normalized* for samples on silicon (with or without an oxide layer) by acquiring an image of the Raman scattering from the silicon substrate. An image at ~950 cm^{-1}, the second order silicon Raman peak,[1] can be easily obtained with our tunable filter, and follows the profile of the laser. Then, the Raman image of graphene can be normalized by dividing the two images (after subtracting the dark background from each) with image processing software, as shown below.

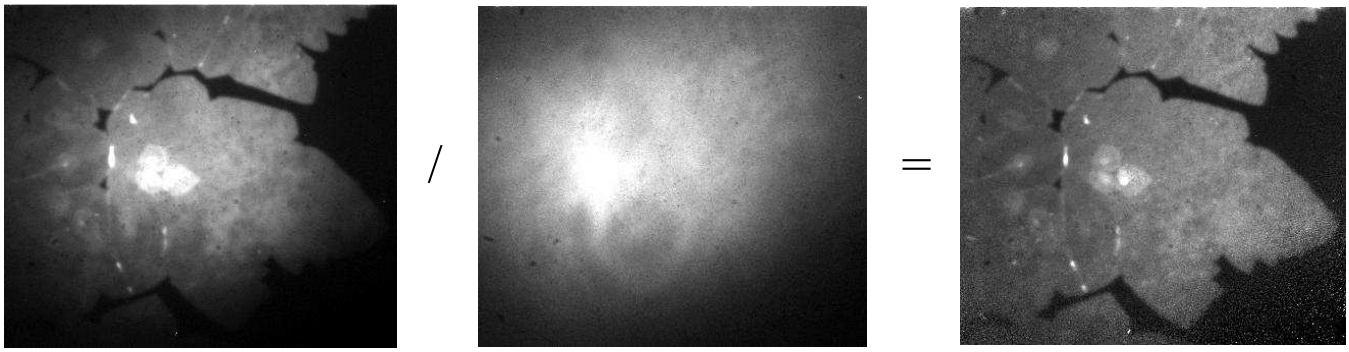

Figure S3: Illustration of procedure for image normalization. A G band image (left, from Figure 2 in main text) is divided by an image of the silicon substrate Raman scattering (center), which is proportional to laser intensity, to give a normalized image (right).

Copper exhibits a relatively strong luminescence background with respect to the graphene Raman signal,[2, 3] but it is low enough for an excitation wavelength of 450 nm that WRI of graphene on copper is still possible. However, we find that for the G band image, the contrast flips, and single-layer graphene appears darker than the bare substrate (Figure S4). Collecting Raman spectra at adjacent locations on and off the graphene (laser intensity roughly constant) shows that near the G peak, the background is slightly higher off the graphene than on the graphene, accounting for the contrast flip when integrated over the range of our bandpass filter (~10 nm, Thorlabs) (Figure S5). A 2D/G ratio

image (calculated analogously to Figure S3) provides the highest contrast, and has the additional benefit of being automatically normalized with respect to laser intensity.

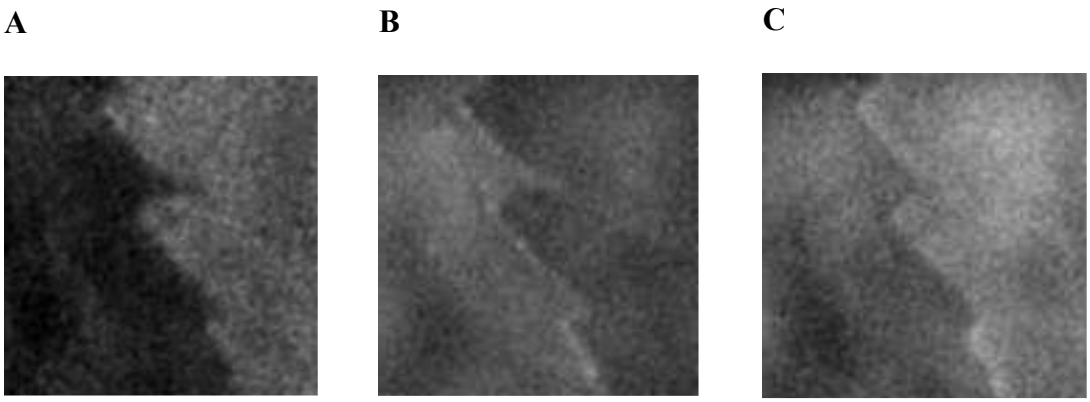

Figure S4: (A) 2D/G ratio image of graphene on copper (from Figure 3A in main text). Graphene appears brighter than copper substrate. (B) Raw G band image of graphene on copper, showing contrast flip. (C) Raw 2D band image of graphene on copper. As in (A), the graphene appears brighter than the substrate. (B) and (C) were each acquired in 5 minutes.

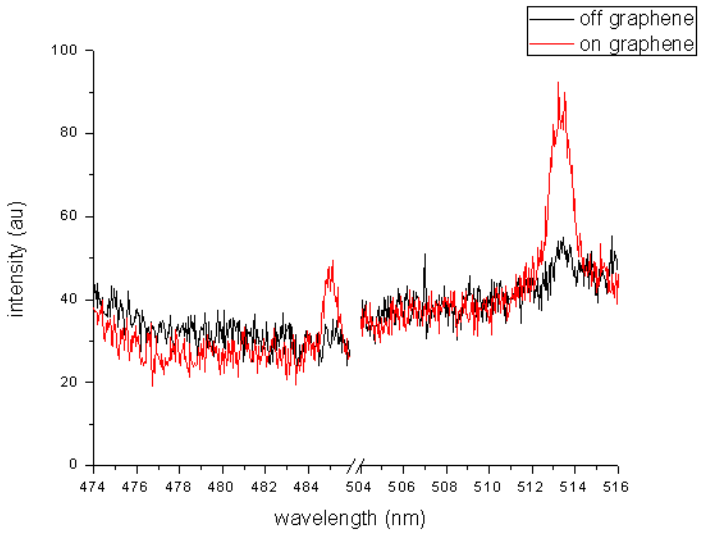

Figure S5: Raman spectra on and off graphene on copper over the wavelength range of the G (left) and 2D (right) bandpass filters, after subtracting dark background. The integrated Raman signal (copper background + G band) over the range of the G bandpass filter (~475-485 nm) is slightly higher off the

graphene, accounting for the contrast flip in the G band image.

Dark-field TEM imaging

Dark-field TEM imaging of graphene was performed using the procedure outlined by Huang *et al*.[4] Selected area diffraction of the graphene results in sets of six-fold symmetric diffraction spots, with each set of spots corresponding to a different crystallographic orientation of graphene within the selected area. Using an objective aperture to select a specific diffraction spot forms a dark-field image of only the graphene which is within a small range of crystallographic orientations. The region in Figure 5B was identified as multi-layer because it appeared in two dark-field images corresponding to two well-separated diffraction spots (the layers had different crystallographic orientations).

Because dark-field imaging is sensitive to crystallinity, it is possible that the circular features we see could correspond to regions of amorphous material, rather than etch pits. However, the size and homogeneous diameter distribution of these features is similar to the etch pits identified with AFM on multi-layer oxidized graphene by Liu *et al.*,[5] leading us to believe that the origin of these features is the same in both cases.

Tearing suspended graphene (video caption)

Attached video shows suspended graphene tearing, induced by 50 mW laser power. Laser is initially at a lower (25 mW) power, and graphene stays intact. Power is increased to 50 mW at t = 2.5 sec, causing a hole to form in the graphene film. Moving the sample eventually causes the hole to propagate, destroying the graphene film starting at t = 17 sec. All images are Gaussian blurred (radius 1 pixel = 125 nm) to reduce CCD noise. Speed is 4x real time.

References

1. Parker, J.; Feldman, D.; Ashkin, M., Raman scattering by silicon and germanium. *Physical Review* **1967,** *155* (3), 712-714.
2. Boyd, G.; Yu, Z.; Shen, Y., Photoinduced luminescence from the noble metals and its

enhancement on roughened surfaces. *Physical Review B* **1986,** *33* (12), 7923-7936.
3. Zhao, L.; He, R.; Rim, K.; Schiros, T.; Kim, K.; Zhou, H.; Gutierrez, C.; Chockalingam, S.; Arguello, C.; Palova, L.; Nordlund, D.; Hybertsen, M.; Reichman, D.; Heinz, T.; Kim, P.; Pinczuk, A.; Flynn, G.; Pasupathy, A., Visualizing Individual Nitrogen Dopants in Monolayer Graphene. *Science* **2011,** *333* (6045), 999-1003.
4. Huang, P.; Ruiz-Vargas, C.; van der Zande, A.; Whitney, W.; Levendorf, M.; Kevek, J.; Garg, S.; Alden, J.; Hustedt, C.; Zhu, Y.; Park, J.; McEuen, P.; Muller, D., Grains and grain boundaries in single-layer graphene atomic patchwork quilts. *Nature* **2011,** *469* (7330), 389-392.
5. Liu, L.; Ryu, S.; Tomasik, M.; Stolyarova, E.; Jung, N.; Hybertsen, M.; Steigerwald, M.; Brus, L.; Flynn, G., Graphene oxidation: Thickness-dependent etching and strong chemical doping. *Nano Letters* **2008,** *8* (7), 1965-1970.